Reclamation of salt-affected land by total ponding with drainage: Numerical simulations for different soils and different drainage system configurations

Nguyen, P. H. T., Chapuis, R. P. & Millette, L.
Département des génies civil, géologique et des mines – École Polytechnique, Montréal, QC, Canada.

ABSTRACT
In agricultural areas, reclamation of salt-affected lands can be done with a total ponding method with drainage. This involves ponding water over the soil surface and leaching salts from the root zone towards an underground drainage system. In this paper, this method is tested using numerical simulations for sands, non-plastic silts and non-swelling, fine-grained soils with low plasticity. The numerical solutions approximate the treatment duration depending on chosen restoration objectives, hydraulic conductivity of soils and configuration of the drainage system (depth, spacing). They assume an absence of organic matter and neglect adsorption and diffusion, which exposes their limitations.

RÉSUMÉ
En zone agricole, la restauration de sols salins peut se faire avec une méthode par inondation totale avec drainage. Ceci signifie d'inonder la surface du sol pour lessiver les sels de la zone racinaire vers un système de drainage souterrain. Dans cet article, cette méthode est testée en utilisant des simulations numériques pour les sables, les silts non plastiques et les sols fins peu plastiques et non gonflants. Les solutions numériques approximent la durée du traitement en fonction des objectifs de restauration choisis, de la conductivité hydraulique du sol et de la configuration du système de drainage (profondeur, espacement). Elles supposent une absence de matière organique et négligent l'adsorption et la diffusion, ce qui expose leurs limites.

1 INTRODUCTION

Salinization in arable lands is the accumulation of soluble salts in the root zone. It occurs mainly in arid or semi-arid regions, where water resources and rainfall are insufficient to effectively leach salts out from the root zone. In these climates, a high water table and rapid evaporation of moisture near the surface contribute jointly to precipitation and accumulation.

The salts are mostly sulfate, chloride, carbonate or bicarbonate (Sheaffer and Moncada, 2011). They come from the weathering of geological formations naturally rich in salts, an aquifer recharged by seawater or human activity, such as the use of salt-rich irrigated water (Ayers and Westcot, 1985).

Negative impacts of excessive salinization include soil erosion and limited plant growth, leading to low crop productivity and economic loss. On a yearly basis, around 2500 to 5000 km^2 of arable lands are lost from production worldwide due to build-ups of salts (FAO, 2002). This issue is expected to continue and to intensify under the adverse effects of climate change. Along with a growing world population, restorative measures become necessary to meet increasing food demands.

One such measure is the leaching by total ponding with drainage. The latter consists in flooding the entire contaminated surface with water, which leads to vertical infiltration, solubilization of solid salts and leaching of solutes towards a subsurface drainage system. While simple in its application, this method encompasses preferential pathways for water flow and solute transport in areas near drains (Siyal et al. 2010). It is also susceptible to water loss through evaporation at the pond's surface.

This paper evaluates the efficiency of the total ponding method under varying parameters. The latter are soil permeability, depth of drains (z_d), spacing between them (L) and chosen restorative goals, which are based on the proportion of salts eliminated (P) and the targeted depth to decontaminate (z). Homogeneous cases, as well as cases with a drainage layer, are under scrutinity.

This investigation is accomplished with numerical simulations using the GeoStudio software, which performs finite element analyzes of groundwater flow (Seep/W) and solute transport (Ctran/W) in a 2-D porous media. From numerical solutions, leaching curves are constructed for sands, non-plastic silts and non-swelling, cohesive soils with low plasticity.

2 MATHEMATICAL FRAMEWORK AND ESTIMATIONS

Flow regime in a porous media is based on Darcy's law (eq. 1) and the conservation equation (eq. 2) formulated by Richards (1931) :

$$\mathbf{v} = -\mathbf{k}\,\mathrm{grad}\,h \qquad [1]$$

$$\mathrm{div}(\mathbf{k}\,\mathrm{grad}\,h) + Q = \partial\theta/\partial t \qquad [2]$$

where $\mathbf{v}$ is Darcy's velocity vector, $\mathbf{k}$ is the hydraulic conductivity matrix, h is the hydraulic head, Q is a source or sink term, θ is the volumetric water content and t is

time. Eq. 1 and 2 are both valid for saturated and unsaturated flow.

k and θ are functions of u_w, where k is the unsaturated hydraulic conductivity and u_w is the pore-water pressure. They define the unsaturated behaviour of soils. The water retention curve $\theta(u_w)$ is estimated using the modified Kovács (MK) model, which provides practical means to approximate $\theta(u_w)$ using simple equations and basic geotechnical properties. The complete set of equations for both granular and plastic-cohesive soils are given by Aubertin et al. (2003).

For an isotropic medium, the off-diagonal entries of the matrix $\mathbf{k}$ are zero, while the main diagonal entries equal $k(u_w)$. The latter is estimated from $\theta(u_w)$ with the equations of van Genuchten (1980) :

$$k = k_s \frac{\left[1-(au_w^{(n-1)})(1+(au_w^n)^{-m})\right]^2}{\left[((1+au_w)^n)^{\frac{m}{2}}\right]} \quad [3]$$

$$n = 1/(1-m) \quad [4]$$

$$S = \frac{1}{(\theta_s-\theta_r)}\left|\frac{d\theta_p}{d(\log(u_p))}\right| \quad [5]$$

$$m = 1-\exp(-0.8S) \text{ for } 0 \le S \le 1 \quad [6]$$

$$m = 1-0.5755/S+0.1/S^2+0.025/S^3 \text{ for } S > 1 \quad [7]$$

$$a = \frac{1}{u_w}\left(2^{\frac{1}{m}}-1\right)^{(1-m)} \quad [8]$$

k_s is the saturated hydraulic conductivity. a, n and m are adjustment parameters. S, θ_p and u_p are respectively the slope, the volumetric water content and the water pressure at the halfway point between θ_s and θ_r on the water retention curve. θ_s and θ_r are respectively the saturated and the residual volumetric water contents.

An approximate value of k_s is given using predictive methods. For granular soils including non-plastic silts, Chapuis (2004) gives an estimation of k_s with the following empirical equation :

$$k_s = 2{,}4622\left(\frac{d_{10}^2 e^3}{1+e}\right)^{0.7825} \quad [9]$$

where k_s is in cm/s, d_{10} (mm) is the grain size at 10% passing and e is the soil void ratio. Eq. 10 gives good results for natural soils in the following ranges: 0,003 ≤ d_{10} ≤ 3 and 0,3 ≤ e ≤ 1.

For plastic soils, Mbonimpa et al. (2002) propose the following predictive equation :

$$k_s = C_p \frac{\gamma_w}{\nu_w}\frac{e^{3+x}}{(1+e)}\frac{1}{\rho_s^2 w_L^{2x}} \quad [10]$$

where k_s is in cm/s, $C_p = 5.6\ g^2/m^4$, γ_w is the water unit weight (9.8 kN/m^3), ν_w is the dynamic viscosity of water (10^{-3} Pa·s), X =1.5, ρ_s is the density of solids (kg/m^3), w_L is the liquid limit (%) and $x = 7{,}7 w_L^{-0.15} - 3$.

For solute transport problems, the governing general equation is (Wexler, 1992) :

$$\partial C/\partial t = -\text{grad}\,[vC - \mathbf{D}\cdot\text{grad}\,C] + Q_s \quad [11]$$

where C is the concentration of solute, $\mathbf{D}$ is the hydrodynamic dispersion matrix and Q_s is a source or sink term for production or loss of solute within the system. Eq. 11 is the advection-dispersion equation, assuming no sorption or decay reactions.

For 2-D flow, matrix $\mathbf{D}$ is defined by (Bear, 1979) **:**

$$\begin{bmatrix} D_{11} & D_{12} \\ D_{21} & D_{22} \end{bmatrix} \quad [12]$$

where :

$$D_{11} = \alpha_L\frac{v_x^2}{v} + \alpha_T\frac{v_y^2}{v} + D^* \quad [13]$$

$$D_{22} = \alpha_T\frac{v_x^2}{v} + \alpha_L\frac{v_y^2}{v} + D^* \quad [14]$$

$$D_{12} = D_{21} = (\alpha_L - \alpha_T)\frac{v_x v_y}{v} \quad [15]$$

$$|v| = \sqrt{v_x^2 + v_y^2} \quad [16]$$

D_{11}, D_{22}, D_{12} and D_{21} are hydrodynamic dispersion coefficients. α_L and α_T are respectively the longitudinal and transverse dispersivities. $|v|$ is the norm of Darcy's velocity vector. v_x and v_y are respectively average linear flow velocities in the x and y directions, and D^* is the coefficient of molecular diffusion.

In field experiments, values of α_L range approximately from 0.1 to 2 m over short transport distances and may exceed 10 m for large-scale distances. Values of α_T are at least an order of magnitude smaller than α_L (Gelhar et al. 1992; Domenico and Schwartz, 1997).

3 SOIL CHARACTERIZATION

Soil selections are aimed to cover a range of different hydraulic properties. The chosen range is a value of k_s varying from about 10^{-4} m/s to 10^{-8} m/s.

Five soils are studied and identified by letters A to E. Soils A and C are sands, while soils B and D are non-plastic silts. Soil E is a non-swelling, fine-grained material with a low plasticity. Its liquid limit is 15%, which corresponds to a silty clay or clayey silt according to Casagrande (1948). For plastic soils, it should be noted that w_L, e and ρ_s are the only geotechnical properties necessary to estimate $\theta(u_w)$ and k_s, with the MK model and eq. 10 respectively. For all soils, geotechnical data are provided in table 1. Table 2 lists the saturated hydraulic conductivity obtained with predictive methods. Figures 1 and 2 illustrate $\theta(u_w)$ and $k(u_w)$ estimated respectively with the MK model and the van Genuchten model.

Table 1. Geotechnical data

Parameter	A	B	C	D	E
d_{10} (mm)	0,135	0,008	0,250	0,012	-
d_{60} (mm)	0,210	0,063	5,000	0,050	-
Cu(-)	1,6	7,9	20,0	4,2	-
Clay (%)	1,0	0,0	0,0	0,0	-
Silt (%)	2,5	73,0	2,5	70,0	-
Fine sand (%)	94,5	27,0	16,5	28,0	-
Medium sand (%)	2,0	0,0	23,0	2,0	-
Coarse sand (%)	0,0	0,0	17,0	0,0	-
Gravel (%)	0,0	0,0	41,0	0,0	-
w_L(%)	-	-	-	-	15
USCS class.	SP	ML	SW	ML	CL-ML
Porosity	0,5				
Void ratio (e)	1				
ρ_s (kg/m^3)	2700				

Table 2. Predicted k_s

Id	Soil type	k_s (m/s)
A	Granular soil / non-plastic silt (eq. 9)	6,23E-04
B		7,48E-06
C		1,64E-03
D		1,41E-05
E	Plastic soil (eq. 10)	1,12E-08

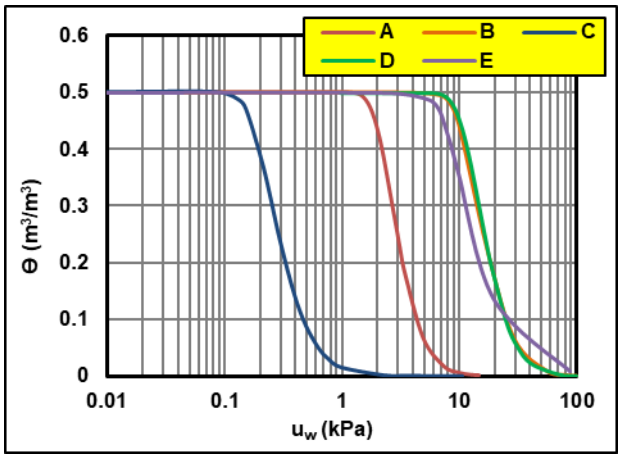

Figure 1. Water retention curves $\theta(u_w)$

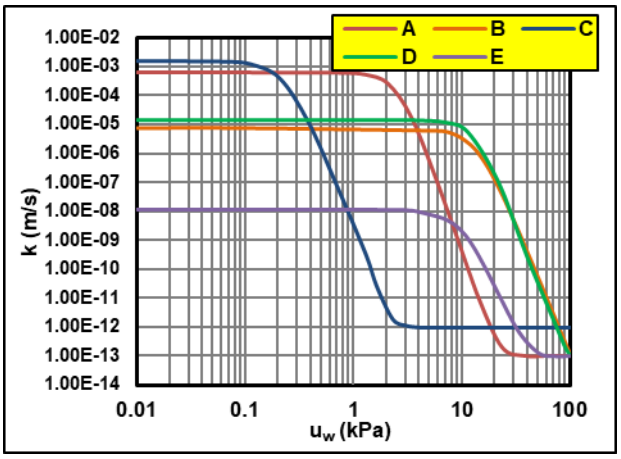

Figure 2. Permeability curves $k(u_w)$

4 DESCRIPTION OF THE NUMERICAL MODEL

The numerical model consists of a two-dimensional section of 1,25 m in height, as shown in figure 3. Two types of sections are observed, i.e. homogeneous cases and cases with a drainage layer.

In homogeneous cases, the stratigraphy is as follows: a layer of 1.1 m of the studied soil followed by an underlying layer of clay (k_s= 1 X 10^{-12} m/s). The latter has a thickness of 0.15 m. A half circle with a radius of 5 cm represents the drain at a depth of 0,6 m, 0,8 m or 1,0 m depending on the case. For cases with a drainage layer, a 5 cm thick permeable material is added at drain level, taking the full horizontal length of the section.

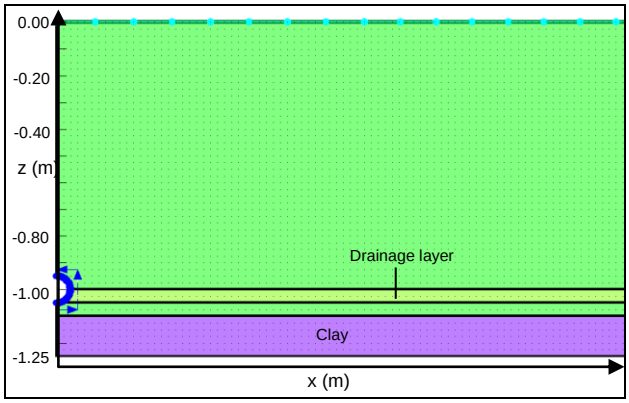

Figure 3. Geometry example with a drainage layer

Modelling parameters, such as boundary conditions, are explained in the following sections.

4.1 Initial conditions and boundary conditions

Initial conditions assume a groundwater table lowered by underground drains. A pressure head of 0 kPa is therefore applied to the drain and the soil is fully saturated initially. In order to mimic a total pond and initiate water infiltration in a transient regime, a hydraulic head of 1 cm

is applied at ground level. Evidently, a steady-state regime is achieved when saturation is reached.

Also, a homogeneously contaminated underground is assumed initially, i.e. salt content stays the same throughout the soil before leaching. In saturated soil, initial salt concentration is set at 100 % or 100 g/m^3. In unsaturated soil, dilution occurs during water infiltration. Therefore, initial concentration in unsaturated soil is expressed as :

$$C_i = (C_s \times \theta_s)/\theta \quad [17]$$

where C_i is the initial salt concentration in unsaturated soil (g/ m^3), C_s is the initial salt concentration in saturated soil (100 g/m^3) and θ is the *in situ* volumetric water content (m^3/m^3).

During the transient and steady-state regimes, an exit boundary condition is applied to the drain, allowing extraction of water and solutes.

In the modelling software, implementing eq. 17 requires subdividing the unsaturated soil into several horizontal layers (see figure 4). This geometry is most important for soils where low capillary rise is expected, since the vadose zone is thinner in this case.

Each layer is associated with the average concentration calculated between two elevations geometrically delimiting said layer. The thinner these layers are, the better the model reproduces eq. 17, as shown in figure 5 for soil A.

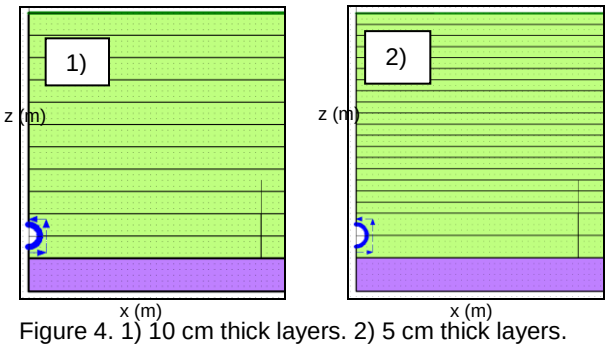

Figure 4. 1) 10 cm thick layers. 2) 5 cm thick layers.

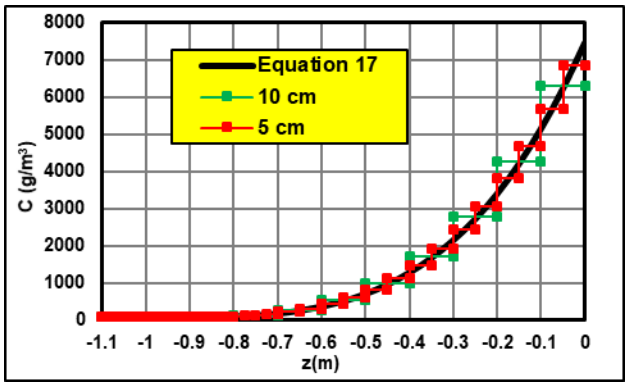

Figure 5. Initial concentration for soil A

Effects of layer thickness on leaching results were investigated on soil A for a homogeneous case with a drain located at a depth of 1 m. Two numerical analyzes were carried out, one with layers of 10 cm (case #1) and another with layers of 5 cm (case #2). Using the same mesh and time steps, flow regime stayed the same for the two cases.

It was found that relative difference in salt concentration $C(x,z,t)$ between cases #1 and #2 decreased as saturation increased. It remained below 4% once a steady-state regime was achieved (Nguyen, 2017). The difference was thus considered negligible. In this paper, all models are done with 10 cm thick layers.

4.2 Solute transport hypothesis

Numerical models assume the following simplifying assumptions:

- The media is isotropic;
- Molecular diffusion is neglected;
- Adsorption is neglected;
- Longitudinal and transverse dispersivities are respectively 2 m and 0.2 m.

Consequences of those hypotheses are explained in the discussion.

5 DATA GATHERING AND RESULTS

Raw numerical results provide concentrations (C) in time (t) and space (x, z). This paper therefore compiles values of $C(x,z,t)$ to construct leaching curves, which are in fact isoconcentration lines. The latter express the time necessary to leach a fixed proportion (P) of contaminants at a constant depth (z) and at different spacing between drains (L). C is expressed as:

$$C = C_s * (1 - P) \quad [18]$$

where P is the proportion of salts eliminated. P acts as a restoration objective and is expressed as:

$$P = 1 - X/Y \quad [19]$$

where X is the final electrical conductivity after leaching and Y is the initial electrical conductivity before leaching. Both X and Y are determined in saturated conditions and can be expressed in terms of salt concentration, since electrical conductivity and salt concentration are roughly correlated by a linear regression (USSLS, 1954). X depends on restoration objectives and can be based on the salt tolerance of a specific culture.

Since flow regime is symmetrical in respect to a plane located halfway between two drains, spacing between them is expressed as:

$$L = 2M \quad [20]$$

where L is the spacing between drains and M is the length of the model parallel to the abscissa x.

Table 3 summarizes the parameters of all constructed numerical models, the results of which are compiled to draw leaching curves in figures 6 and 7.

Table 3. Summary of numerical models

Model name	Soil	Drainage layer	t_{TR} (s)	t_L (d)	Q_{SAT} ($m^3/s/m$)
Case_1_z_d=-0.6m	A	-	98	11	6.8E-4
Case_1_z_d =-0.8m			213	11	7.7E-4
Case_1_z_d =-1.0m			340	11	7.5E-4
Case_2_z_d =-0.6m	B	-	1	101	8.2E-6
Case_2_z_d =-0.8m			3	101	9.2E-6
Case_2_z_d =-1.0m			52	111	9.0E-6
Case_2_100_z_d =-0.6m		A	1	11	2.7E-5
Case_2_100_z_d =-0.8m			4	11	3.0E-5
Case_2_100_z_d =-1.0m			71	11	3.3E-5
Case_2_1000_z_d =-0.6m		C	34	11	4.2E-5
Case_2_1000_z_d =-0.8m			36	11	4.8E-5
Case_2_1000_z_d =-1.0m			101	11	5.2E-5
Case_3_z_d =-0.6m	E	-	2900 (0.03d)	984	1.2E-8
Case_3_z_d =-0.8m			69000 (0.80d)	985	1.4E-8
Case_3_z_d =-1.0m			379000 (4.39d)	988	1.4E-8
Case_3_100_z_d =-0.6m		B	5600 (0.06d)	1105	1.0E-7
Case_3_100_z_d =-0.8m			87200 (1.01d)	1101	1.2E-7
Case_3_100_z_d =-1.0m			463200 (5.36d)	1106	1.4E-7
Case_3_1000_z_d =-0.6m		D	4800 (0.06d)	1000	1.5E-7
Case_3_1000_z_d =-0.8m			86400 (1d)	1001	1.7E-7
Case_3_1000_z_d =-1.0m			462400 (5.35d)	1006	1.8E-7

z_d : drain depth, t_{TR} : Transient regime duration, t_L : leaching duration reached, Q_{SAT}: Flow rate in one drain in a steady-state regime.

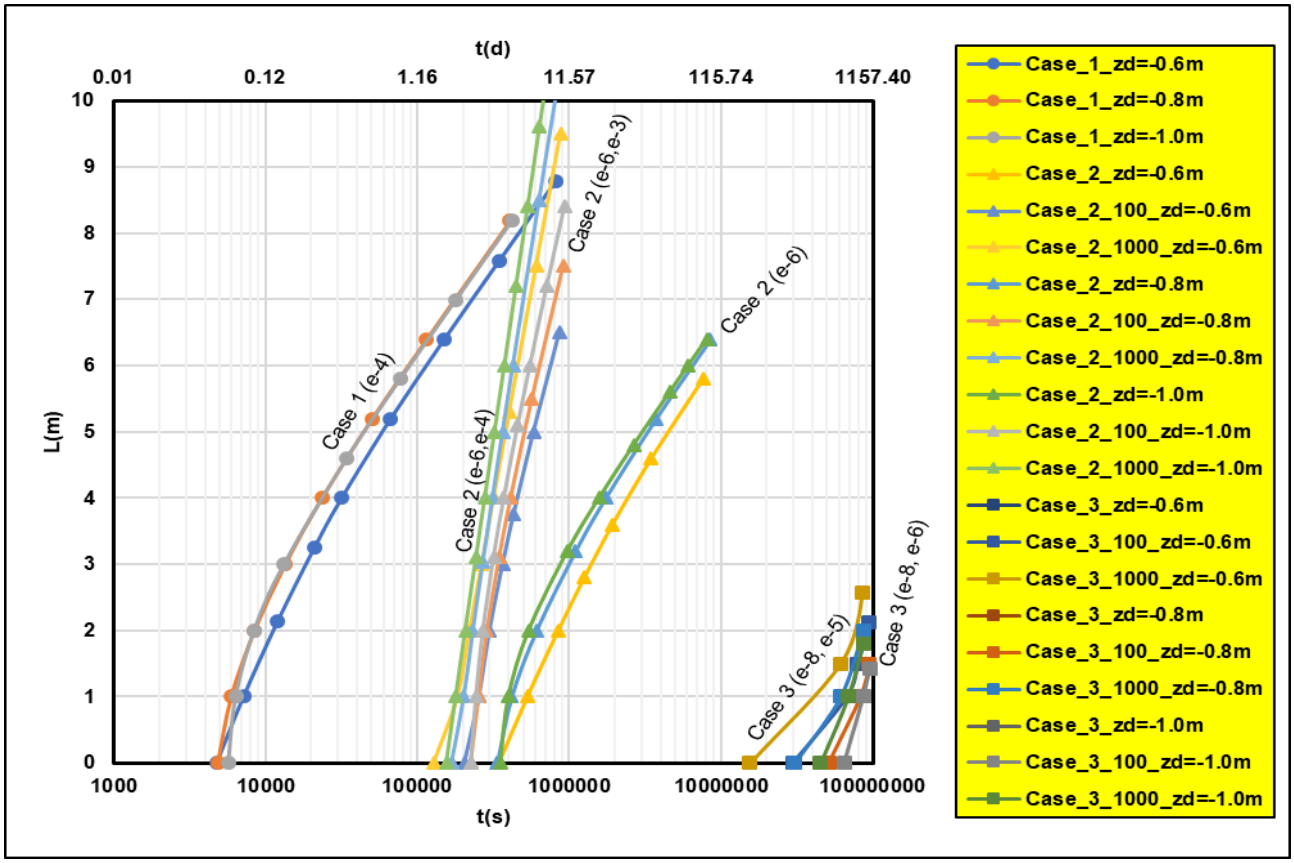

Figure 6. Chart for P = 0,8 and z = -0,5m

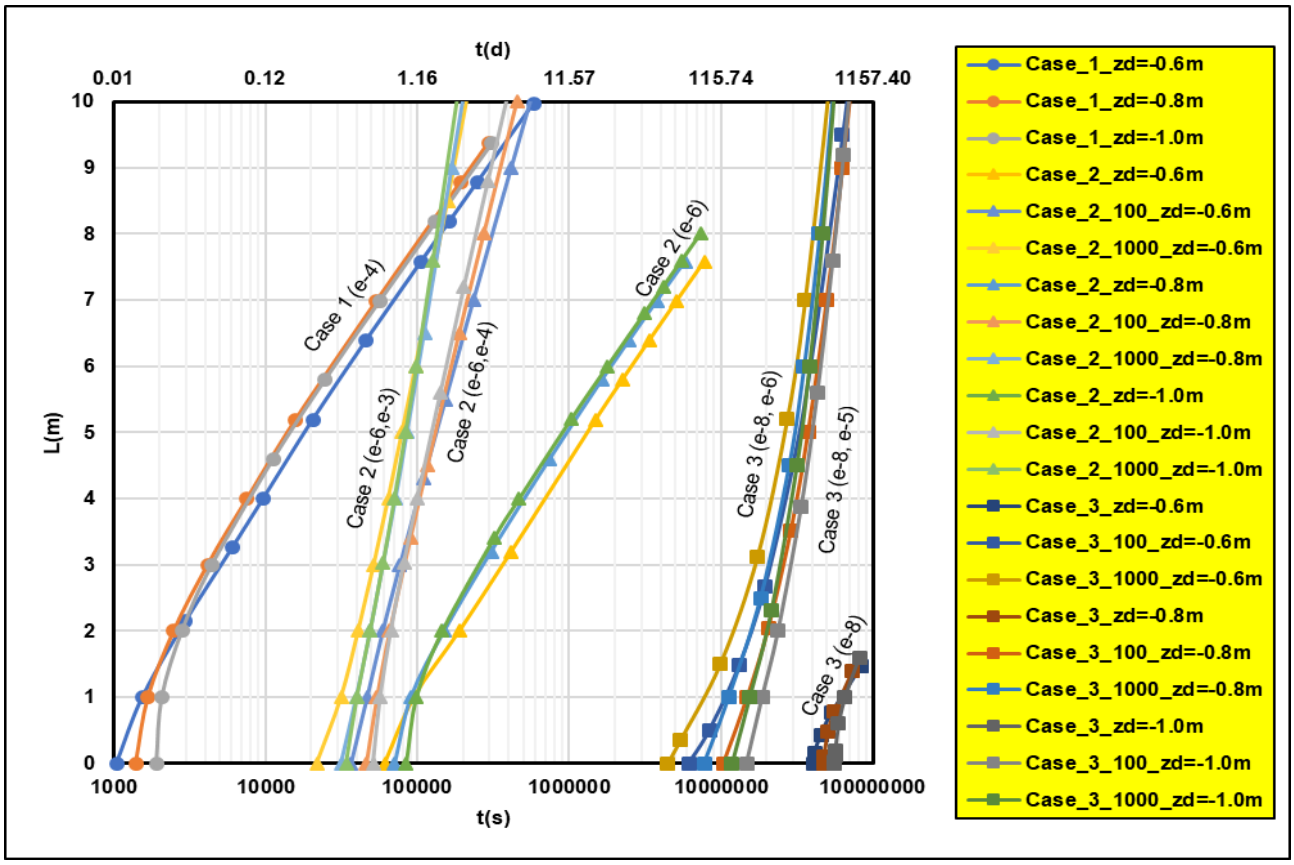

Figure 7. Chart for P = 0,5 and z = -0,3m

Three cases are studied and numbered from 1 to 3. Case # 1 presents a homogeneous permeable soil, i.e. soil A. Cases # 2 and # 3 respectively analyze soil B and E, and each has two cases with a drainage layer : one with a permeability contrast of about 2 orders of magnitude (100) and the other of 3 orders (1000). Figures 6 an 7 are two examples of numerical results produced for values (P, z) of (0.8 ; -0.5 m) and (0.5 ; -0.3 m) respectively. They are part of a set of 15 charts produced by Nguyen (2017), whose work comprises leaching curves built for P values of 0.5, 0.6, 0.7, 0.8 and 0.9, z_d values of -0.6 m, -0.8 m and -1.0 m, and z values of -0.1 m, -0.3 m and -0.5 m. Nguyen (2017) also attempted numerical simulations on a cracked soil, but efforts were fruitless as the software does not allow a heterogeneous porosity in the same medium.

On each figure, each case is represented by a family of 3 curves, one for each drain depth z_d. A family is identified according to the case number, followed by the hydraulic conductivity's order of magnitude belonging to the soil and drainage layer (if present). Table 3 lists flow rate Q_{sat} encountered in a single drain depending on the case. An approximation of drained volume is thus given by :

$$V_d = Q_{sat} \times t \qquad [21]$$

where t is duration treatment. Eq. 21 is only valid for calculating volumes in steady-state conditions and becomes more accurate as time increases. Assuming no evaporation is occurring at the water pond's surface, the total volume of water required to decontaminate 1 m^2 of the soil surface is :

$$V_t = \frac{V_d}{L} \qquad [22]$$

6 APPLICATION

The following application evaluates the effects of a 5 cm thick drainage layer on leaching performances regarding case #2 in figure 6. Soil B is thus under investigation, with soils A and C acting as drainage layers (DL) with permeability contrasts of about 2 and 3 orders of magnitude respectively. Values of z and z_d are -0.5 m and -1.0 m respectively. Soil B possesses an initial electrical conductivity (Y) of 10 dS/m, and is intended for a potato cultivation. Since salt tolerance of a potato crop is 4 dS/m (Wentz, 2001), the targeted final electrical conductivity (X) is 2 dS/m. From eq. 19 :

$$P = \left(1 - \frac{2\ dS/m}{10\ dS/m}\right) = 0.8$$

Figure 5 shows the values of t(L) implemented in eq. 21 and 22 to illustrate, in figure 8, values of V_t. From the

latter, the most economical solutions in terms of water consumption are listed in table 4.

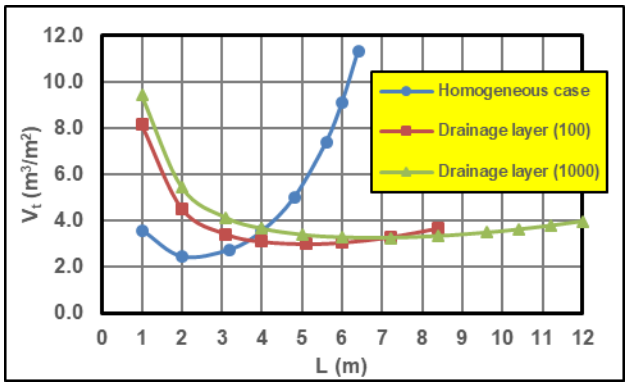

Figure 8. V_t for case #2 (P = 0.8, z = -0.5 m, z_d = -1.0 m)

Table 4 : Optimal solutions

Case type	L(m)	t(s)	V_t (m³/m²)
Homogeneous	2.2	579645 (6.7d)	2.4
DL (100)	5.1	458660 (5.3d)	3.0
DL (1000)	7.0	434151 (5.0d)	3.2

On a side note, drainage system configuration does not depend solely on desired leaching performances. It also depends on drainage performances targeted during crop seasons, which is not taken into account in this paper. Furthermore, installation of a drainage layer is unrealistic, since excavation of the entire land is required. This involves additional costs and soil remoulding. Therefore, the present paper merely explores the idea of a drainage layer and does not investigate further concerning the feasibility of its application.

7 DISCUSSION

Numerical simulation of the total pond is mostly a linear problem, since solute transport is done without adsorption and soil is saturated, except at the beginning of treatment. Leaching curves thus differ mainly according to a single constant, which is k_s.

For homogeneous cases, soils with k_s of 10^{-4}, 10^{-6} and 10^{-8} m/s require respectively a few hours to a few days, a day to a few dozen days and a few hundred days of treatment.

Solutions from table 4 suggest that optimal usage of a drainage layer reduces treatment duration and the number of drains necessary, but at the cost of increased volumes of water needed to leach the same amount of salts. Compared to the homogeneous case #2 in table 4, drainage layers with permeability contrasts of 2 and 3 orders of magnitude require respectively 25% and 33% more water, as well as 21% and 25% less time to achieve the same result. While not verified, similar percentages are expected for case #3, since permeability contrasts and the curves' logarithmic behaviour are similar for both cases #2 and #3.

According to Darcy's law, flow rate varies linearly with z_d in saturated conditions. However, this is not true for z_d = - 1.0 m due to the nearby clay, which has a depth of -1.1 m. This low permeability layer decreases flow velocities around the lower half of the drain and therefore has the negative effect of reducing flow rate. For homogeneous cases, the flow difference is thus minimal between drain depths of -0.8 m and -1.0 m (see Q_{SAT} in table 3). For this reason, the leaching curves at these two depths are hardly distinguishable in the charts. Naturally, curves associated with a drain depth of -0.6 m indicate higher leaching duration, since the flow rate is smaller at this depth. For a constant value of L, a drain depth of -0.6 m requires up to 50% more time to leach the same amount of salt compared to drain depths of -0.8 m and -1.0 m.

Evidently, as z and P increase, the longer treatment takes. When all other parameters remain constant, treatment duration increases by 10% to 30% per increase of 20 cm on z. It increases by a factor of 1.2 to 2.0 for every additional increase of 0.1 on P (Nguyen, 2017).

While the charts provide a quick general portrait of the total ponding method, there are certain limitations associated with the simplifying assumptions. These limitations are treated in the following sections.

7.1 Adsorption

Since adsorption is ignored in numerical models, the latter assume an electrochemically neutral soil. Soils therefore contain no organic matter and no clay mineral particles, whose presence increases cation exchange capacity of soil and thus its adsorbent capacity. The models also make no distinction between the different ions responsible for salinization (Na^+, Ca^{2+}, Mg^{2+}, etc.), which influence adsorption by their valence and concentration in solution. This shortcoming is irrelevant only if the soil has no adsorbent capacity.

Certain conditions may justify the absence of organic matter. Indeed, salinity disrupts microorganisms by decreasing their ability to absorb nutrients. Sensitive microorganisms eventually die and tolerant genotypes have to bear an additional metabolic burden, which reduces bacterial activity (Manpreet, 2012). In the absence of microorganisms, the soil structure becomes fragile and easily damaged by wind, rain and sun. This leads to soil erosion and leaching of nutrients through runoffs of rainwater. As a result, organic matter reserves and biomass production decrease, and the decrease in the bacterial population accelerates (Bot and Benites, 2005). Eventually, soil becomes uncultivable and devoid of organic matter, which are the assumed conditions of the numerical models in this paper.

The absence of clay minerals is justified for cases #1 and #2, because they study granular soils and silts. However, case #3 studies a fine-grained soil that may contain clay minerals. Ignoring adsorption in this case is thus a mistake. Leaching curves associated with case #3 remain valid for quantifying salt concentration in solution, but the quantities adsorbed on grain surfaces are not measured.

7.2 Molecular Diffusion

Negligence of molecular diffusion is legitimate for permeable soils in areas near the drain, where flow forces act as the main transport mechanism (advection). It is not legitimate in locations where flow velocities are slow. The models thus ignore diffusion transport halfway between the drains, where flow velocities are slower. This shortcoming becomes greater with increasing spacing between drains. The numerical models also do not take into account diffusion transport between the contaminated soil and the low permeability clay floor, where concentration gradients are the greatest; initial conditions assume an absence of contaminants in the clay layer.

7.3 Other Limitations

The models presented in this paper assume an environment in which hydraulic conductivity adopts an isotropic behaviour, dispersivities remain constant and initial contamination is homogeneous. While solutions were achieved with satisfactory numerical convergence, the use of homogeneous parameters does not match field conditions, where porosity, permeability, dispersivities and contamination are spatially variable.

In field conditions, macropores are left behind by decomposing roots, creating preferential pathways for water flow and solute transport. Furthermore, a fully saturated soil under a total pond is unrealistic. By the phenomenon of cessation, one can only hope a maximum degree of saturation (Sr) situated between 85% and 90% in field conditions. The flow is then in a steady-state regime, but unsaturated. Leaching is thus not effective in a proportion of 10 to 15% of the total porosity. With Sr = 100% in numerical models, the latter present optimistic scenarios compared to cases encountered in the field.

Other discrepancies include the negligence of solubilization duration in numerical models and the lack of validation with experimental evidence, as no physical model was constructed and no field investigation was conducted.

8 CONCLUSION

Desalinization is crucial to recover arable lands, but requires an effective method that is economically and environmentally viable. This paper draws a general portrait of the total ponding method and provides a framework under which one can evaluate its efficiency with a set of charts. It should be understood that the charts merely offer an approximation of a solution and a general grasp of the total pond's effectiveness under varying parameters, namely soil permeability, L, P, z and z_d.

9 REFERENCES

Aubertin, M. Mbonimpa, M. Bussière, B. and Chapuis, R. P. 2003. A model to predict the water retention curve from basic geotechnical properties. *Canadian Geotechnical Journal*, 40(6), 1104-1122.

Ayers, R.S. and Westcot, D. W. 1985. Water quality for agriculture. *FAO irrigation and drainage paper*, 29 Rev.1.

Bear, J. 1979. *Hydraulics of Groundwater*. McGraw-Hill, London, England.

Bot, A. and Benites, J. 2005. The importance of soil organic matter. *FAO Soils Bulletin*, 80.

Casagrande, A. 1948. Classification and Identification of Soils. *Transaction*, ASCE, 113, 901-930.

Chapuis, R. P. 2004. Predicting the saturated hydraulic conductivity of sand and gravel using effective diameter and void ratio. *Canadian Geotechnical Journal*, 41(5), 787-795.

Darcy, H. 1856. *Les fontaines publiques de la ville de Dijon : exposition et applications des principes à suivre et des formules à employer dans les questions de distribution d'eau*, Victor Dalmont, Paris, France.

Domenico, P. A. and Schwartz, F. W. 1997. *Physical and Chemical Hydrogeology*, 2nd ed., Wiley, Hoboken, NJ, USA.

FAO (Food and Agriculture Organization of the United Nations). 2002. *Crops and Drops: making the best use of water for agriculture*. FAO, Rome.

Gelhar, L. W. Welty, C. Rehfeldt, K. R. 1992. A critical Review of Data on Field-Scale Dispersion in Aquifers. *Water Resources Research*, 28(7), 1955-1974.

Manpreet, S. M. 2012. *Dissolved organic matter dynamics and microbial activity in salt-affected soils*. University of Adelaide, Aidelaide, Australia.

Mbonimpa, M. Aubertin, M. Chapuis, R. P. and Bussière, B. 2002. Practical pedotransfer functions for estimating the saturated hydraulic conductivity. *Geotechnical & Geological Engineering*, 20(3), 235-259.

Nguyen, P.H.T. 2017. *Modélisation numérique de la désalinisation des terres agricoles par inondation complète et drainage*. University of Montreal, Polytechnique Montreal, Montreal, Quebec, Canada.

Richards, L. A. 1931. Capillary conduction of liquids through porous medium*. Physics*, 1, 318-333.

Sheaffer, C. C. and Moncada, K. M. 2011. *Introduction to Agronomy: Food, Crops and Environment*, 2nd ed., Delmar, Clifton Park, NY, USA.

Siyal, A.A. Skaggs, T.H. van Genuchten, M. T. 2010. Reclamation of Saline Soils by Partial Ponding: Simulations for Different Soils. *Vadose zone Journal*. 9: 486-495.

USSLS (United States Salinity Laboratory Staff). 1954. *Diagnosis and Improvement of Saline and Alkali Soils*. United States Department of Agriculture, USA.

van Genuchten, M. T. 1980. A closed–form equation for predicting the hydraulic conductivity of unsaturated soils. *Soil Science Society of America Journal*, 44(5), 892-898.

Wentz, D. 2001. *Salt Tolerance of Plants*. Gov. of Alberta, Canada.

Wexler, E. J. 1992. *Analytical Solutions for One-, Two-, and Three-Dimensional Solute Transport in Ground-Water*. United States Geological Survey, USA.